Supporting Information

Ionic liquids self-combustion synthesis of BiOBr/Bi$_{24}$O$_{31}$Br$_{10}$ Heterojuctions with exceptional visible-light photocatalytic performances

Fa-tang Li,*[ab] Qing Wang,[a] Jingrun Ran,[b] Ying-juan Hao,[a] Xiao-jing Wang,[a] Dishun Zhao[c] and Shi Zhang Qiao*[b]

[a]College of Science, Hebei University of Science and Technology, Shijiazhuang 050018, China.

[b]School of Chemical Engineering, University of Adelaide, Adelaide, SA 5005, Australia.

[c]College of Chemical and Pharmaceutical Engineering, Hebei University of Science and Technology, Shijiazhuang 050018, China.

Table S1 The pseudo-first order rate constants k for 50 mg/L of RhB degradation under visible light irradiation over various catalysts

Sample	Fitted equation	k (min^{-1})	Correlation coefficient (R)
BiOBr	y = 0.0287x + 0.0921	0.0287	0.9834
90%BiOBr	y = 0.0875x + 0.1154	0.0875	0.9927
85%BiOBr	y = 0.0964x + 0.1625	0.0964	0.9802
75%BiOBr	y = 0.1150x + 0.1590	0.1150	0.9878
71%BiOBr	y = 0.0676x + 0.2269	0.0676	0.9986
51%BiOBr	y = 0.0434x + 0.2383	0.0434	0.9947
31%BiOBr	y = 0.0388x + 0.2446	0.0388	0.9845
P25 TiO_2	y = 0.0080x + 0.0070	0.0080	0.9844

Table S2 The pseudo-first order rate constants k for 30 mg/L of MO degradation under visible light irradiation over various catalysts

Sample	Fitted equation	k (min^{-1})	Correlation coefficient (R)
BiOBr	y = 0.0013x + 0.0790	0.0013	0.9983
90%BiOBr	y = 0.0052x + 0.2446	0.0052	0.9997
85%BiOBr	y = 0.0088x + 0.2095	0.0088	0.9800
75%BiOBr	y = 0.0117x + 0.3065	0.0117	0.9976
71%BiOBr	y = 0.0048x + 0.3369	0.0048	0.9983
51%BiOBr	y = 0.0042x + 0.3439	0.0042	0.9984
31%BiOBr	y = 0.0034x + 0.2705	0.0034	0.9961
P25 TiO_2	y = 0.00002x + 0.0030	0.00002	0.9999

Table S3. Electronegativity, calculated CB and VB edge positions of BiOBr and $Bi_{24}O_{31}Br_{10}$ semiconductors.

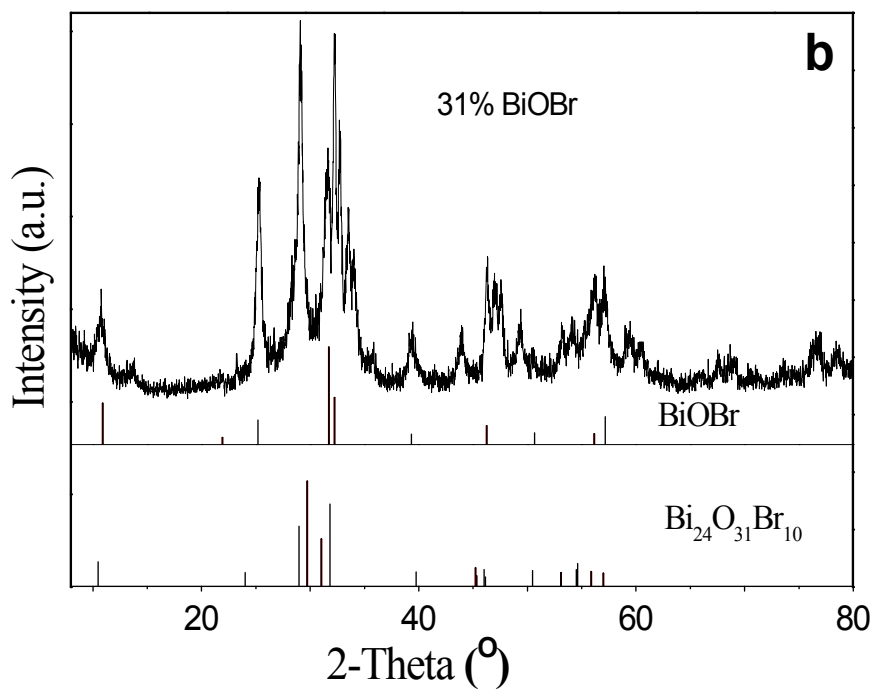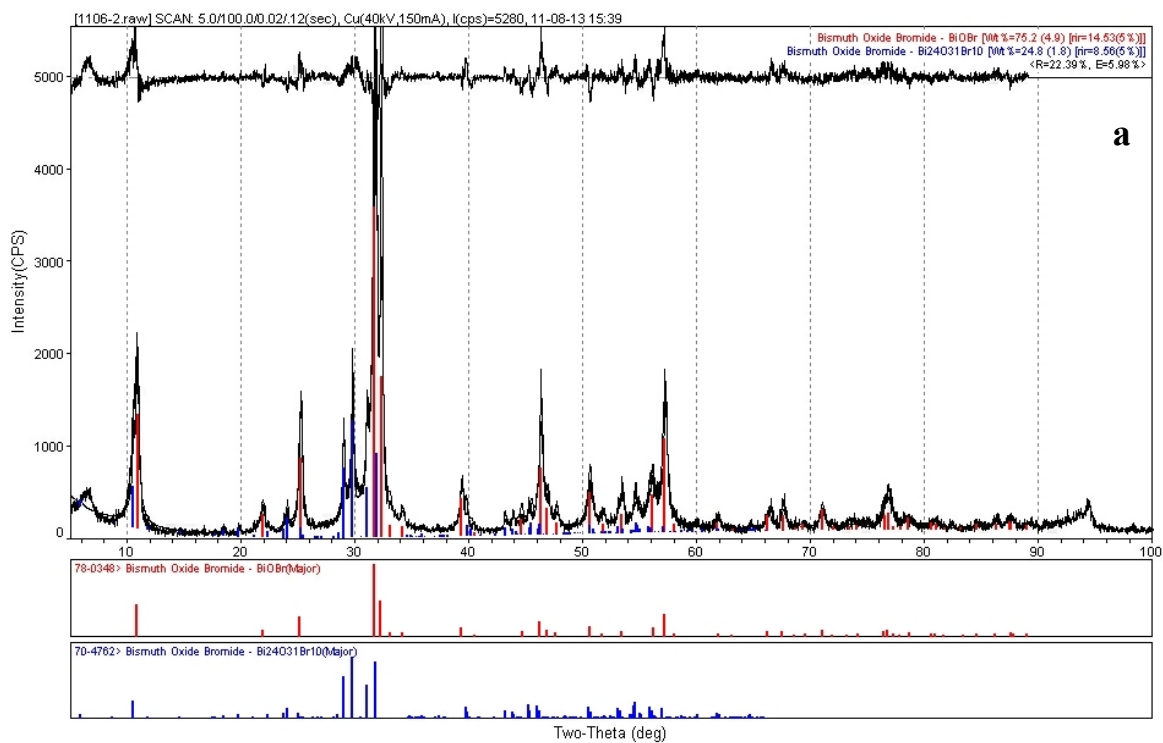| Semiconductor	Eg /eV	Electronegativity (χ) /eV	Calculated CB position /eV	Calculated VB position /eV
BiOBr	2.74	6.17	0.30	3.04
$Bi_{24}O_{31}Br_{10}$	2.52	6.03	0.27	2.79

Fig. S1. (a) XRD patterns showing the composition calculation of heterojunction 75%BiOBr, and (b) XRD patterns of 31%BiOBr.
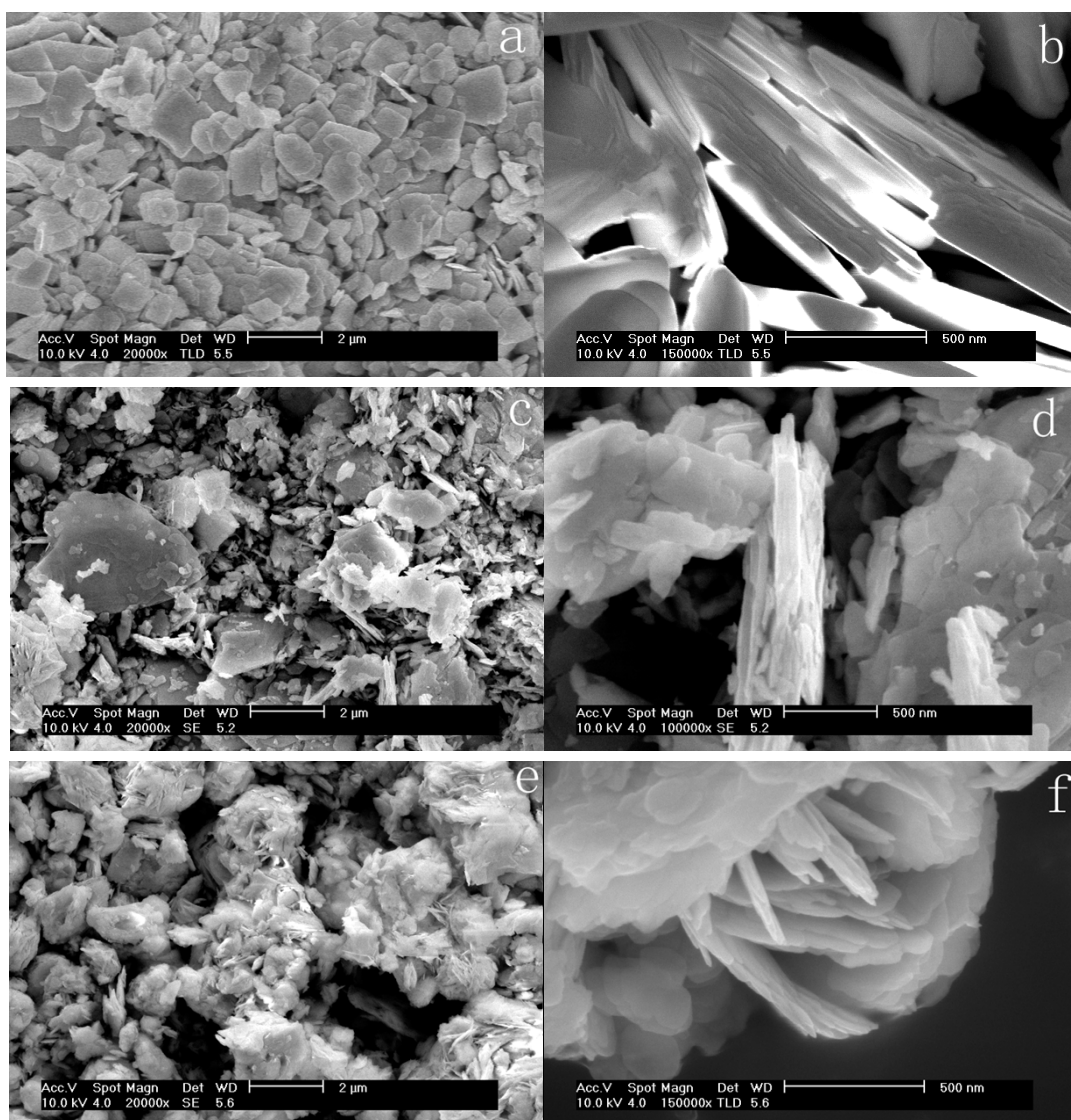
Fig. S2. SEM photographs (a) and (b) of pure BiOBr, (c) and (d) of 75%BiOBr, (e) and (f) of 31%BiOBr.
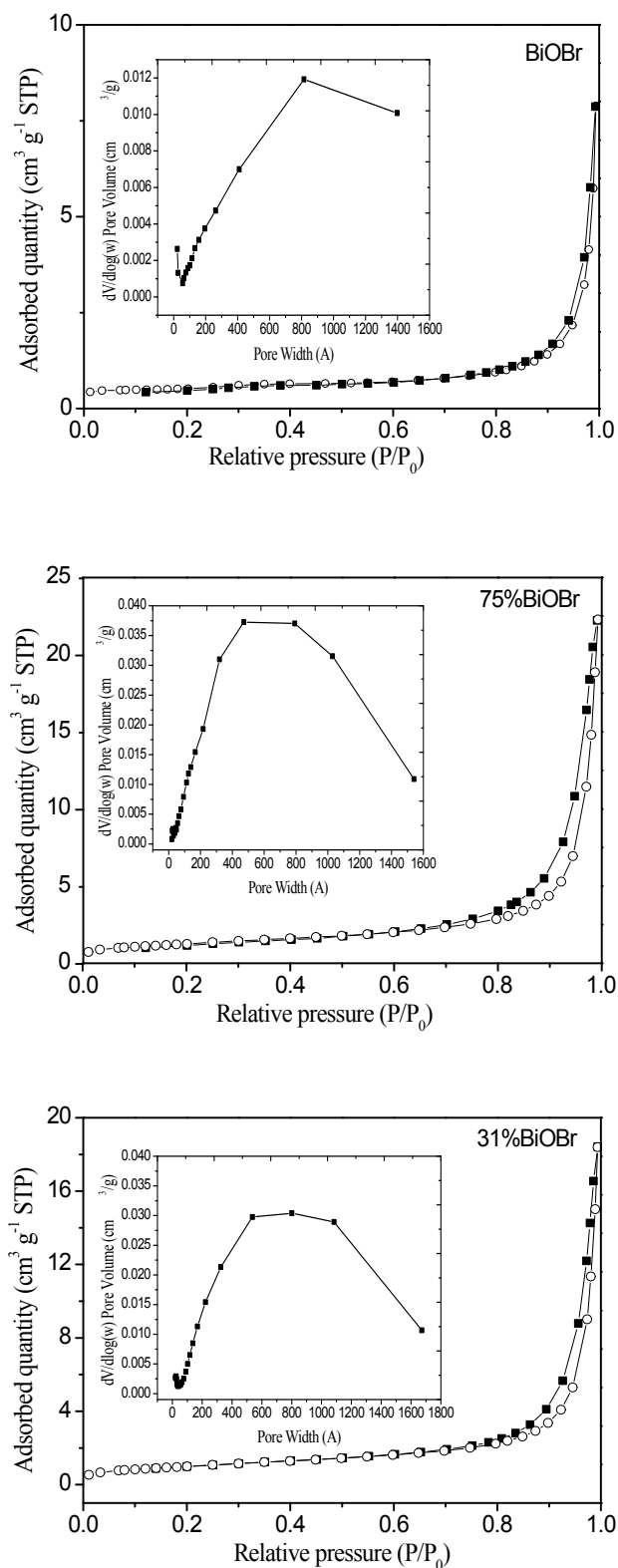
Fig. S3. N_2 absorption-desorption isotherms and the BJH desorption cumulative pore volume curves (inset) of pure BiOBr, 75%BiOBr and 31%BiOBr.
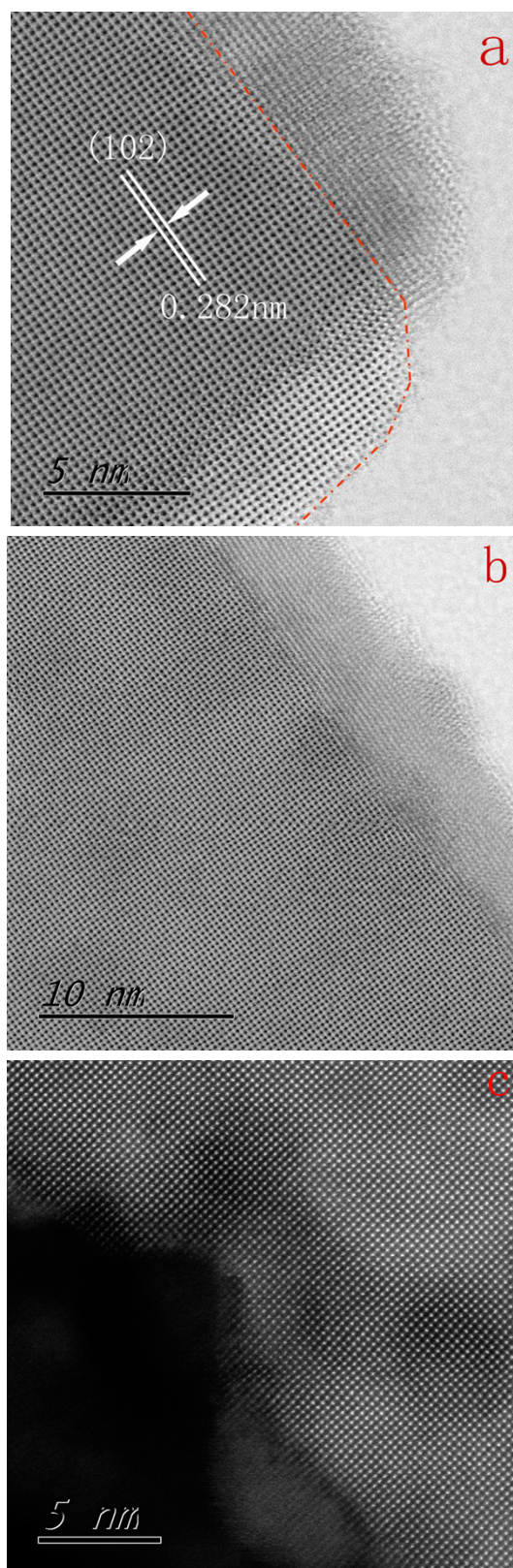
Fig. S4. (a) and (b) ABF STEM images, and (c) HAADF STEM image of the sample 75%BiOBr.
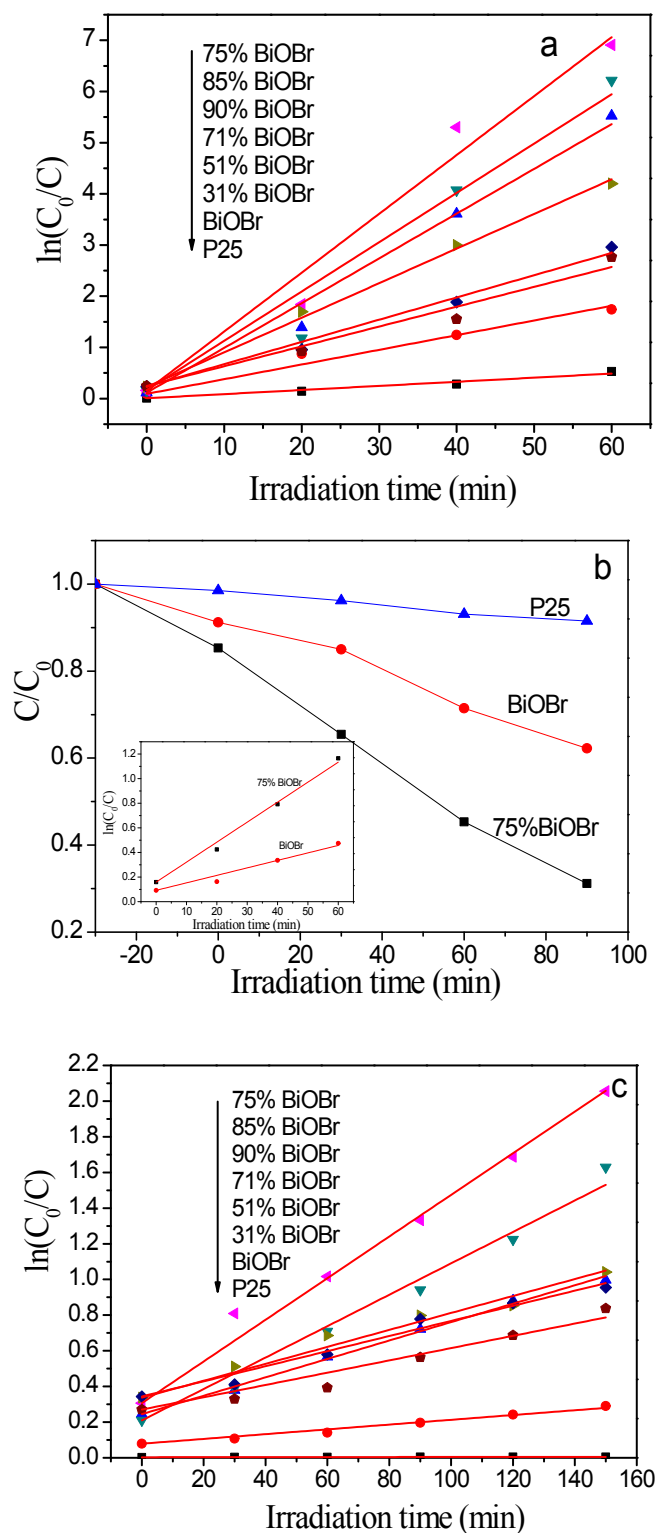
Fig. S5. (a) Time-course variation of $\ln(C_0/C)$ of RhB; (b) time-course variation of C/C_0 and $\ln(C_0/C)$ (inset) of 50 mg/L RhB under 420 nm single wavelength irradiation over 75% BiOBr, pure BiOBr, and P25 TiO_2; and (c) time-course variation of $\ln(C_0/C)$ of MO solution over various photocatalysts.

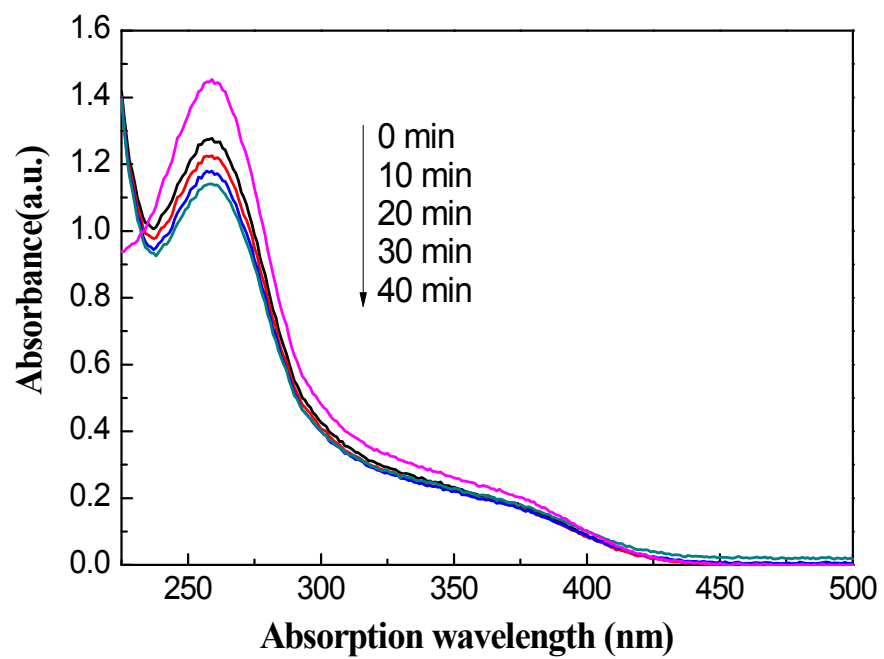**Fig. S6.** Appearance photographs of the samples before and after adsorption of MO and RhB.

Fig. S7. UV-Vis absorption spectra of NBT in 75%BiOBr suspension under the irradiation of λ> 420 nm wavelength.